Chapter 25
Interaction of Laser Radiation with Explosives, Applications and Perspectives

Yuriy Tverjanovich, Andrey Tverjanovich, Anatoliy Averyanov, Maksim Panov, Mikhail Ilyshin and Mikhail Balmakov

Abstract This chapter provides a brief overview of the main directions in research and application of the interaction of laser radiation with explosives. Historically the first application of such interaction based on thermal initiation of explosives is briefly characterized. The main methods of remote detection of explosives using laser radiation are listed. Particular attention is paid to the areas of research that have been recently formed such as spectral selective resonance interaction of laser radiation with explosives and explosives modified by nano-additives. It was noted that depending on the choice of the optical absorption band of the explosives, its excitation can lead either to the effective activation of an explosive or to its decomposition, which is not accompanied by a significant thermal effect. The latter case can be used for remote detection of the explosives and, partly, for passivation of their surface. Finally, it was demonstrated that the absorbing and refractive light nano-additives are able to reduce the threshold intensity of initiation of explosives by laser radiation, while keeping the resistance of explosives to impact or thermal effects that provides the safety conditions of working with them.

Y. Tverjanovich (✉) · A. Tverjanovich · A. Averyanov · M. Panov · M. Balmakov
Institute of Chemistry, St. Petersburg State University, Universitetskiy ave. 28, St. Petersburg, Russia
e-mail: y.tveryanovich@spbu.ru

A. Tverjanovich
e-mail: andr.tver@yahoo.com

M. Panov
e-mail: m.s.panov@spbu.ru

M. Balmakov
e-mail: balmak1@yahoo.com

M. Ilyshin
St. Petersburg State Institute of Technology, Moskovsky ave. 26, St. Petersburg, Russia
e-mail: explaser1945@yandex.ru

K. Yamanouchi et al. (eds.), *Progress in Photon Science*, Springer Series in Chemical Physics 119, https://doi.org/10.1007/978-3-030-05974-3_25

25.1 Introduction

The first experiments focused on a study of interaction between energy-saturated materials and laser radiation have been performed simultaneously with development of laser technology in the second half of the twentieth century. In most cases, the infrared He–Ne lasers available at that time were applied in this regard. It was assumed that the direct transfer of thermal energy to the substance is provided in the infrared region and, as a result, this is the easiest way to ensure rapid combustion of a substance to be initiated, and subsequent ignition of brisant explosives. The further development of works in this area lies in implementation of high-power lasers for the direct initiation of brisant explosives in order to exclude the necessity to use highly sensitive initiating explosives. However, the use of high-power lasers is difficult to implement and expensive. It was considered that in their absence the probability of accidental initiation of ammo decreases. The number of works on laser initiation of energy-saturated materials has increased several times over the past ten years, which proves their relevance. The recent success in the understanding of the theory of the initiation process under the action of laser radiation and in the technical development of laser technologies also provide the conditions for further progress of the aforementioned approach. Laser initiation opens wide opportunities for application in those areas where modern safety standards are implemented and restrictions to traditional methods of initiation are presented: space technology and rocket science, mining and blasting with high explosion hazard, oil production, and others. Furthermore, laser initiation makes it possible to create complex explosive systems insensitive to electromagnetic interference and temperature fluctuations and easy to combine into multi-level networks, which makes its application more safe and technological. An additional factor is that the laser initiation process consumes significantly less energy than the thermal type of initiation, in turn, the cost of such initiators is lower than usual ones and their size and weight are also significantly less. For example, the initiation of many pyrotechnic compounds requires low radiation power (mJ), which is accessible for many commercial lasers. Another striking advantage of such initiators is their reusability. At the present, the main approaches describing the process of laser initiation of explosives can be divided into two separate directions: thermal and shock. In the first case, the beam falls on the target causing a self-sustaining combustion process, which then proceeds into explosive combustion or detonation. In the second case, the detonation occurs due to the energy of shock initiation caused by particles flying at high speed, which are formed upon laser radiation.

One more actual and perspective way of using lasers is the methods of detecting various substances. There are a lot of different laser methods for detection of energetic materials. But traditional detection methods are somewhat limited because the broad spectral features of many explosive vapors make phase sensitive detection methods difficult. One of the common problems of a large part of these methods is the following. Large molecules, which include the majority of explosives, usually have

weak and poorly resolved optical transitions. This circumstance complicates their detection by spectroscopic methods. At present, remote sensing of energy-saturated substances using resonant laser-explosives interactions is a promising direction of solving this problem.

Another modern directions in the field of interaction of laser radiation with explosives are using resonant laser-explosive interaction and nanoparticle additives. Introduction to the explosive composition some chemically inactive nanoparticles can reduce the threshold power of initiation by laser radiation. The low chemical activity of these nanoparticles allows to achieve this goal without reducing the stability and safety of the explosives.

In the sections below, an overview of the research in this direction will be reviewed.

25.1.1 Laser Thermal Initiation of Explosives

In many modern studies, it was observed that ignition or initiation of materials by laser radiation result in thermal inhomogeneity of the process, which is manifested by formation of hot spots [1]. It is assumed that during irradiation a local center of about 0.1 μm is formed, which has enough energy to ignite an initiator. For that reason, the temperature of hot spot should be approximately 700 °C or more, and its lifetime should be not less than 10 μs. There is a possibility to form a number of such hot points; however, formation of a "critical" hot spot induces detonation or ignition. The process of thermal initiation consists of a complex of different physical and chemical stages. For example, the initiation process of hexogen (RDX—Royal Demolition Explosive, Hexogen) can be described as follows [2–4]. In the beginning, the surface of the sample is heated by a laser beam (at atmospheric pressure in argon with CO_2 laser heat flux from 35 to 600 W/cm^2) and the temperature profile of the material in the solid phase is formed. Then, when the material reaches melting temperature (T_m), a quasi-equilibrium two-phase zone (mushy zone) is formed, in which both the solid and liquid phases are present. Further, the molten liquid phase is formed, which moves deep into the material and transfers thermal energy. This process accompanied by decomposition and formations of gaseous phase.

In the next stage, a torch is formed on the surface of the material followed by the intense evaporation of gaseous products from the surface of the material and subsequent sharp increase in pressure. Finally, if the heat flux is strong enough to provide a self-sustaining exothermic reaction, the ignition process occurs (Fig. 25.1).

As a rule, the mathematical modeling methods are used to study the influence of various factors of laser radiation on explosives. Abdulazeem et al. [5] perform theoretical calculations for lead azide using the following mathematical equation:

$$\rho c \frac{\partial T}{\partial t} = k \frac{\partial^2 T}{\partial x^2} + \rho q A e^{-E/RT} + \alpha I(t) e^{-\alpha x},$$

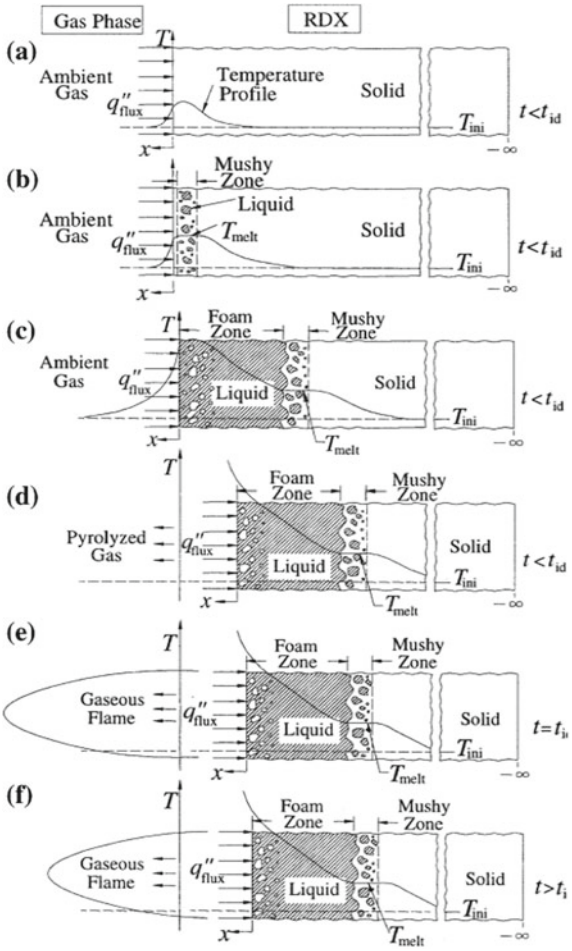

Fig. 25.1 Processes involved in laser-induced ignition of RDX [2]

where, $k\frac{\partial^2 T}{\partial x^2}$—the value of heat transfer taking into account coefficient of thermal conductivity, $\rho q A e^{-E/RT}$—the amount of heat generated during the chemical reaction, $\alpha I(t)e^{-\alpha x}$—the amount of heat produced by laser radiation.

As a result, the dependencies of the surface temperature and the initiation time on the laser radiation density at different values of the heat transfer coefficient were determined (Fig. 25.2a, b). In general, the performed calculations are consistent with the experimental data. In turn, some inconsistency between theory and experiment can be explained by insufficient consideration of an influence of the local zones of the thermal inhomogeneity observed during laser-induced initiation (Fig. 25.2c, d).

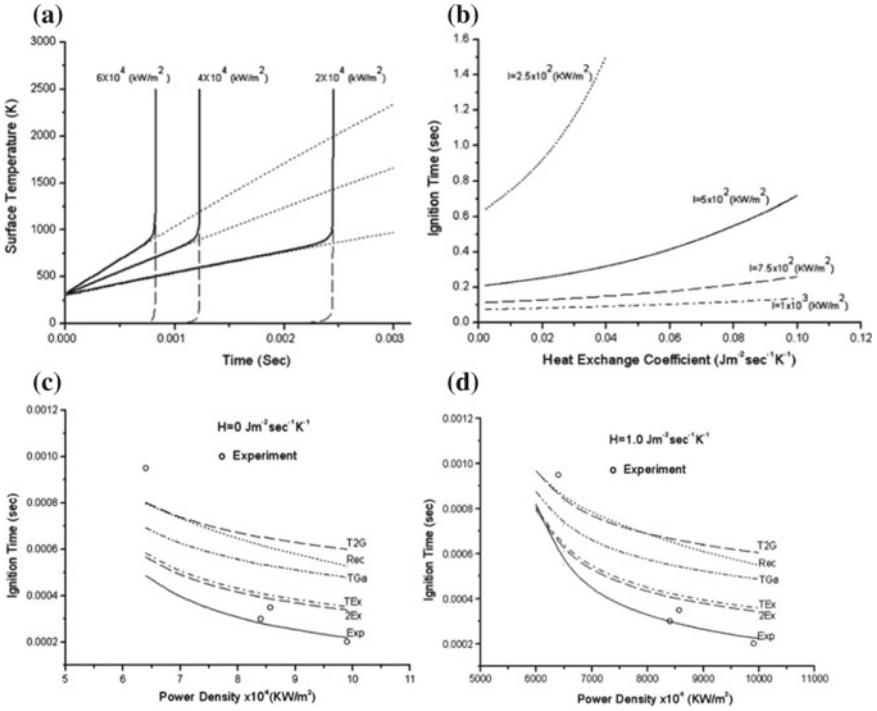

Fig. 25.2 The calculated and obtained experimentally dependencies of the surface temperature and the initiation time on the laser radiation density at different values of the heat transfer coefficient [5]

25.1.2 Laser Shock Initiation of Explosives

The well-known alternative way to initiate explosives is to use the energy of plasma produced during laser ablation of a metal. The shock wave generated by the flying particles directed on the initiating explosive creates an inertial impact that transforms into a detonation front. Typically, a metal coating is made of a thin metal film placed on the transparent "window" or tip of the optical fiber. The laser pulse (Nd:YAG laser, laser energy 67–375.7 mJ) vaporizes the metal and forms a plasma. In the implementation of this mechanism of initiation of hexogen (RDX), octogen (HMX), trinitrotoluene (TNT), and hexanitrostilbene (HNS) the following processes occur: melting and evaporation of a metal, plasma formation, shock wave formation, and, finally, detonation of an explosive. In this case, the main materials used as target are aluminum and copper. For fabrication of multilayer films based on carbon, magnesium, germanium, titan, titan oxide, aluminum oxide, and zinc sulfide are also used [6].

25.2 Detection of Explosives Using Laser Irradiation

25.2.1 Main Laser Methods of Explosives Detection

Currently, methods for the remote detection of the energy-saturated substances is a perspective direction in the modern security strategies [7]. There are two approaches applicable for remote detection of explosives. It is standoff detection (fully non-contact method) and remote detection, in which an analytical equipment contacts the sample explosive, whereas an operator is located at a safe distance. Standoff identification of explosives is more promising and demanded, however, more difficult to implement and is limited to low saturated vapor pressures upon normal conditions (e.g., for TNT—9 ppb (~$1.7 \cdot 10^{-3}$ Pa), for RDX—6 ppt (~$4 \cdot 10^{-6}$ Pa)). Moreover, new types of explosives have complicated spectral characteristics and, in the most cases, are poorly studied and the appropriate spectral databases are absent. However, many substances of this class have high adhesion and contain a relatively large trace amount of molecules on the surface per unit area, which facilitates their determination. Modern trends in development of methods and equipment for remote detection are presented below [8].

25.2.1.1 Laser-Induced Breakdown Spectroscopy (LIBS) or Laser Spark Emission Spectroscopy

This method determines the elemental composition of the target substance based on registration of the characteristic lines of emission spectrum of laser plasma [8–12]. For that purpose, the pulsed lasers operating in the UV (area of electronic transitions of most explosives) or IR (area of vibrational-rotational transitions) parts of the spectrum are typically used. For example, the analysis of such explosives as RDX, HMX, TNT, pentaerythritol tetranitrate (PETN), C4, A5, M43, LX-14, and JA2 was successfully performed. Thus, this method has a high sensitivity (nano- and picograms); it is relatively simple and applicable for determination of the most of explosives.

25.2.1.2 Raman Spectroscopy (Spectroscopy of Raman Scattering)

This approach is based on detection of the characteristic Raman spectra of the individual compounds upon laser irradiation [13]. The main disadvantage of this method is insufficient intensity of the scattered radiation of the compounds of interest, which causes the implementation of highly sensitive detectors. In addition, the systems of scanning and accumulation (multiplication) of the signal are required. Moreover, the method is sensitive to external light illumination and luminescence of the object of research and other compounds localized in the scanning zone, which complicates the detection process [14, 15]. In order to increase the intensity of the Raman signal it

is necessary to use the radiation sources in the range of the electronic transitions of molecules (Resonance Raman scattering (RRS)) that allows us to achieve intensity (cross-section of Raman scattering) of thousand times higher than at wavelengths of the visible region for some explosives. For example, in [16] it was shown that the cross-section of Raman scattering at 229 nm for the studied explosives exceeds its value in the visible region of the spectrum by about three orders of magnitude. Gares et al. [17] suggested to use a UV-Raman method, in which the detection occurs right after when molecules of explosive are promoted to the excited state by the UV light. This type of experiments was conducted for TNT, RDX, $NaNO_3$, and NH_4NO_3. It is considered that the optimal distance for remote detection of various explosive compounds using Raman spectroscopy is about 500–1000 m [18].

25.2.1.3 Coherent Anti-Stokes Raman Scattering (CARS) Spectroscopy

This method is based on the phasing molecular vibrations in the field of resonant bi-harmonic pump and subsequent coherent scattering of the probe wavelength [13, 19]. This makes CARS popular for standoff detection of explosive remainders on the surfaces of objects. At the same time, the use of the narrow-band lasers allows achieving high spectral resolution of the Raman bands. Furthermore, CARS has a number of advantages over the method previously discussed, but at the same time, there are difficulties, which complicate its implementation in portable devices designed for remote detection of trace remainders of explosives.

25.2.1.4 Laser-Induced Fluorescence of Products PF-LIF (PD-LIF)

This technique deals with determination of explosives based on the products of their decomposition. In this regard, the analysis is performed by means of detection of the characteristic set of the fragmentation products on the basis of detection of their fluorescence [20–25]. The molecules of the most explosives have weak transitions, whereas the transitions corresponding to the products of their fragmentation are intense and well-studied, therefore, they can be easily identified. The detection process can be divided into two steps: rapid heating and dissociation of the molecules of explosives caused by laser irradiation are followed by the release of a large number of volatile products. As a rule, the spectral characteristics of such decomposition products have simple structure. In the next step, the detection of fluorescence signal of primary decomposition products of explosives as well as their assignment are conducted. This approach has great perspective for further development and with a high degree of probability allows to identify explosives or their mixtures. Here are main advantages of this method: the possibility to use a single source for fragmentation and excitation, high selectivity of detection of functional groups, low influence of optical interference, and relatively intense fluorescence signal.

25.2.1.5 IR Spectroscopy of the Products of Laser Photofragmentation of Explosives (MIR-PF)

This method is based on principles, which are similar to the previous approach differing only in the fact that after irradiation (usually at a wavelength of about 1.5 μm) the registration of gaseous products is carried out using IR spectroscopy. The signal in the form of reflected (scattered) radiation is recorded using IR camera [26–30].

25.3 An Investigation of Laser-Explosive Interaction from New Perspectives

25.3.1 Optimization of Laser Initiation of Explosive—Resonant Laser Explosive Interaction

At the very beginning, research in the field of interaction of laser radiation with photosensitive explosives was largely slowed down by a limited number of high-tech, reliable, powerful, and commercial available lasers. In these conditions, on the one hand, it was technically difficult to find a laser suitable for excitation of the specific absorption bands of an explosive, however, on the other hand, it was useless since the sufficiently powerful laser can initiate almost any explosive. As a result, due to thermal initiation the laser beam interacts with the surface of an explosive by heating it up to a critical temperature [31]. The development of laser technologies and the creation of a wide range of lasers with various characteristics operating at different wavelengths, including those that correspond to the of optical absorption of explosives, provide the conditions for the study of the resonance interaction of laser radiation with explosives.

Thus, it is possible to distinguish two new directions in research of light-sensitive explosives: the resonant interaction with laser radiation and influence of nanoparticles on the mechanism of interaction of explosives with laser radiation.

Here are some aspects of the resonant interaction of explosives with laser radiation. The mechanism of the photo-induced decomposition of HNS (2,2′, 4,4′, 6,6′-hexanitrostillbene) and the resulting decomposition products were studied using UV spectroscopy, electron paramagnetic resonance (EPR), and XPS (X-ray photoemission spectroscopy) [32]. The HNS particles dissolved in acetonitrile were irradiated with a monochromatic source of UV radiation (365 nm) at a temperature of 24 °C. Then, the irradiated HNS was studied using optical absorption spectroscopy within the range of 190–900 nm, as well as X-ray photoemission spectroscopy (XPS) after 2 and 8 h of irradiation. After irradiation, new peaks on the HNS absorption spectrum centered at 330–350 nm appear, the intensity of which increases in proportion to the irradiation time. These peaks are associated with elimination of NO_2-group from the benzene ring of the HNS molecule (Fig. 25.3).

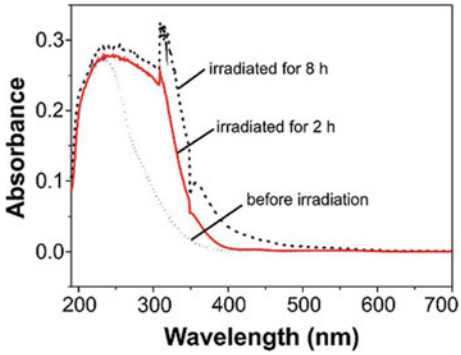

Fig. 25.3 UV-Vis spectra of HNS before and after UV irradiation [32]

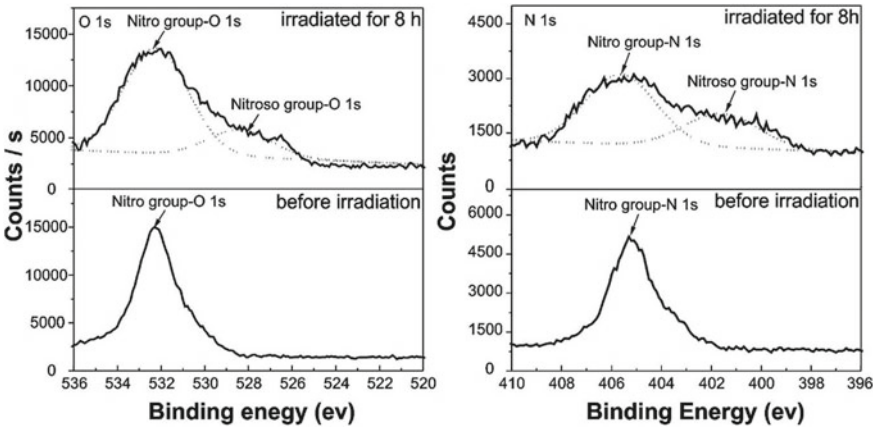

Fig. 25.4 XPS O 1s and N 1s spectra of HNS before and after irradiation, the solid line is the XPS curve and the short dotted line is the fitting curve [32]

The data presented in Fig. 25.3 are confirmed by X-ray photoemission spectroscopy (XPS), electron paramagnetic resonance (EPR), and liquid chromatography-mass spectrometry (LC-MS). The XPS results demonstrate a change in the intensity of peaks N 1s (401 eV) and O 1s (528 eV) when comparing spectra before and after irradiation of HNS. This indicates a breaking of a C–NO_2 bond and the elimination of oxygen from the nitro group (Fig. 25.4). The EPR analysis reveals the presence of free •NO_2 radicals, which are formed during the photocleavage of the C–NO_2 bond in the benzene ring. Thus, the decomposition reaction proceeds mainly through the breaking of a C–NO_2 bond and the elimination of oxygen atoms from the NO_2 groups.

Kakar et al. recorded the absorption spectra (Fig. 25.5) of TATB (triaminotrinitrobenzene or 2,4,6-triamino-1,3,5-trinitrobenzene) before and after irradiation of different intensity (5 min, ~10^{10} photons/s; 5 min, ~10^{14} photons/s), using X-ray

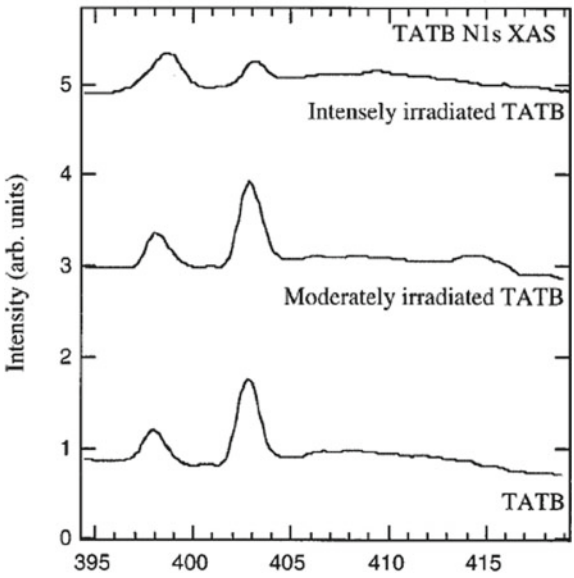

Fig. 25.5 N 1s absorption spectra of TATB recorded at 403 eV: bottom-a fresh TATB film, middle-TATB film exposed to moderate dose of radiation for 5 min, top-TATB film exposed to intense dose of radiation for 5 min [33, 34]

absorption spectroscopy (XAS) [33, 34]. After irradiation, the signals of the transitions N 1s (C–NO_2) → π* (NO), C 1s (C–NO_2) → π* (NO), and O 1s (C–NO_2) → π* (NO) are significantly reduced, which indicates the elimination of the NO_2 group from the benzene ring of the TATB molecule.

Particular interest deserves a study of resonance interaction of laser radiation with cobalt (III) aminates [35–42]. This is due to the fact that these high-energy materials are sensitive to laser radiation, have a high detonation speed (~7 km/s) in comparison with the industrial initiating explosives (e.g., detonation speed for lead azide is 5.5 km/s) [43], have a short area of transition between burning and detonation, and their sensitivity is comparable to the brisant explosives [44]. Thus, all mentioned above make these high-energy materials safe in terms of initiation [45].

Here are the following high-energy materials used in the current study: (5-Nitrotetrazolato-N_2) Pentaammin-Cobalt (III) Perchlorate (NCP); bis-[cis-(5-Nitrotetrazolato–N_2)]}tetraaminecobalt (III) perchlorate (BNCP); (1,5-diaminotetrazole–N_2) pentaamminecobalt (III) perchlorate (DPCP); (5-trinitrometiltetrazole–N_2) pentaamminecobalt (III) perchlorate (TPCP); Aquapentaammincobalt (III) perchlorate (APCP). APCP is used as a precursor for the synthesis of the aforementioned compounds. NCP has successfully passed industrial tests at Geofizika science-and-production company as the main component of the explosion converter in the blasting-perforation equipment applied for drilling of deep oil and natural-gas wells. BNCP is used for space-rocket complexes as one of the most effective explosives.

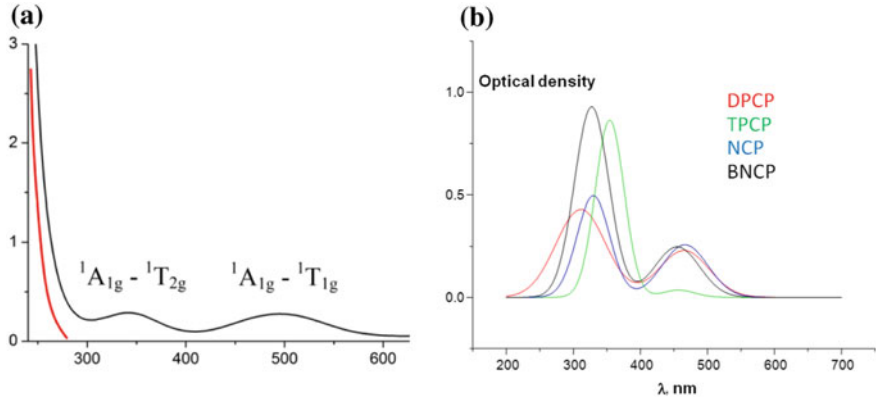

Fig. 25.6 **a** The absorption spectrum of APCP consisting of the charge transfer ligand-to-metal absorption band (highlighted in red) and two d–d absorption bands, **b** The absorption bands corresponding to d–d transitions of other studied cobalt (III) complexes

The 0.022 M aqueous solutions of these complexes were prepared and placed in cuvettes with a volume of 0.2 cm^2 to determine the absorption band frequencies. For example, the absorption spectra of APCP in UV and visible regions [35, 41] consist of the charge transfer metal-to-ligand absorption band and two absorption bands corresponding to the d–d transitions of cobalt (Fig. 25.6a). The d–d absorption bands of other energy-saturated complexes are shown in Fig. 25.6b. Figure 25.6 demonstrates that the third harmonic of the YAG-Nd laser ($\lambda = 355$ nm, pulse duration is 20 ns, pulse frequency 12 kHz, and laser power of 1.2 W) and the semiconductor laser operating at 470 nm (laser power of 0.2 W) can be used for excitation of these bands. In addition, the IR spectra of DPCP, TPCP, BNCP, and NCP were measured (Fig. 25.7) in order to identify the decomposition products [35, 46, 47].

The spectra of all studied complexes are characterized by the following main modes (Fig. 25.7d). One of them are absorption bands associated with vibrations of ClO_4^- ion. These vibrations are characterized by two very intense bands centered at 1070 and 620 cm^{-1}, as well as a weak absorption band centered at 930 cm^{-1} [48]. These absorption bands were observed for all studied complexes. The absorption bands corresponding to vibrations of the intrasphere ligand NH_3 lie in the region of 3200 and 3300 cm^{-1} [49].

Raman spectra of DPCP, TPCP, NCP, and BNCP were recorded for the analogical purpose [36, 38]. Figure 25.8 presents the Raman spectra of NCP and its decomposition producs.

According to Fig. 25.8, there are three intense Raman signals of ClO_4^- centered at 470, 630, and 940 cm^{-1} [50]. These Raman signals were observed for all studied complexes. There are two Raman signals corresponding to vibrations of the intrasphere ligand NH_3 appeared in the region of 1320 cm^{-1} [50–52].

The comparison of the spectra of initial complexes and liquid products of their photolytic decomposition reveals weakening of the intensities of the bands associated

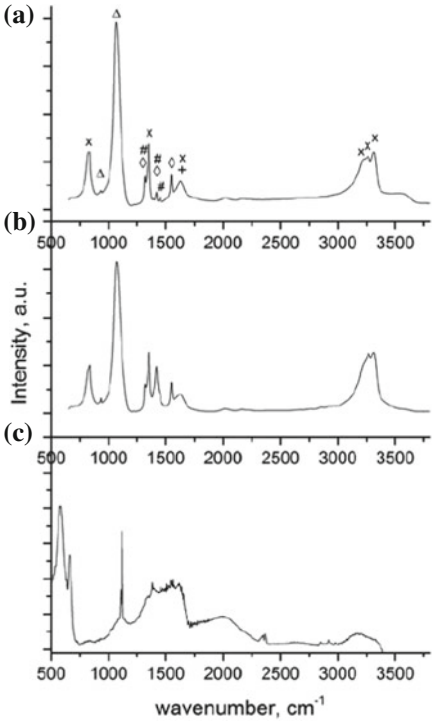

(d) IR (cm^{-1}) Assignment

IR, (cm^{-1})	Assignment
830	NH_3 (x)
934	ClO_4^- (Δ)
1068	ClO_4^- (Δ)
1317	NO_2 (◊), Tz (#)
1353	NH_3 (x)
1421	NO_2 (◊), Tz (#)
1451	Tz (#)
1549	NO_2 (◊)
1629	H_2O (+), NH_3 (x)
3221	NH_3 (x)
3261	NH_3 (x)
3312	NH_3 (x)

Fig. 25.7 **a** IR spectrum of NCP; IR spectra of liquid, **b** and solid, **c** products of photolytic decomposition of NCP upon irradiation at 355 nm, **d** the results of assignment of the obtained IR absorption bands

to intrasphere NH_3 ligand and Co–N, preservation of the intensity of the signals assigned to the outersphere ClO_4 ligand, and the increase in the intensities of the bands corresponding to nitrogen oxides.

In addition to the products remaining in a solution, a solid precipitate is formed because of photolytic decomposition of the complexes. The more detailed study of this precipitate showed that it is composed by cobalt and oxygen forming a mixture of cobalt oxides and hydroxides. Moreover, the increase in the intensity of the light flux leads to decrease of amount of hydroxides in the mixture.

As can be seen from Fig. 25.9, the described above picture is similar in both cases: at 355-nm excitation of the cobalt $^1A_{1g} \rightarrow {}^1T_{2g}$ transition by the third harmonic of the YAG-Nd laser and at 470 nm excitation of the cobalt $^1A_{1g} \rightarrow {}^1T_{1g}$ transition by a semiconductor laser.

The thermal decomposition of cobalt (III) complexes was also studied using mass spectrometry (ionizing radiation 70 eV) [40]. The results of these studies for APCP and NCP demonstrate that the transition from low (150 °C) to high (250 °C) temperatures results in the decrease of the amount of ammonium in the decomposition products, the increase of the average oxidation degree of nitrogen and carbon, and the

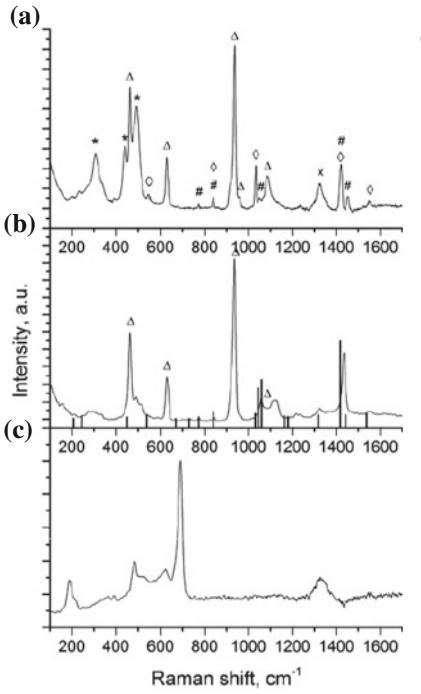

(d)

Raman shift, (cm^{-1})	Assignment
307	Co-N (*)
440	Co-N (*)
463	ClO_4^- (Δ)
494	Co-N (*)
544	NO_2 (◊)
625	ClO_4^- (Δ)
774	Tz (#)
839	Tz (#), NO_2 (◊)
937	ClO_4^- (Δ)
959	ClO_4^- (Δ)
1034	NO_2 (◊)
1053	Tz (#)
1085	ClO_4^- (Δ)
1322	NH_3 (x)
1419	NO_2 (◊), Tz (#)
1453	Tz (#)
1550	NO_2 (◊)

Fig. 25.8 **a** Raman spectrum of NCP; Raman spectra of liquid, **b** and solid, **c** products of photolytic decomposition of NCP upon irradiation at 355 nm, **d** the results of assignment of the obtained Raman bands

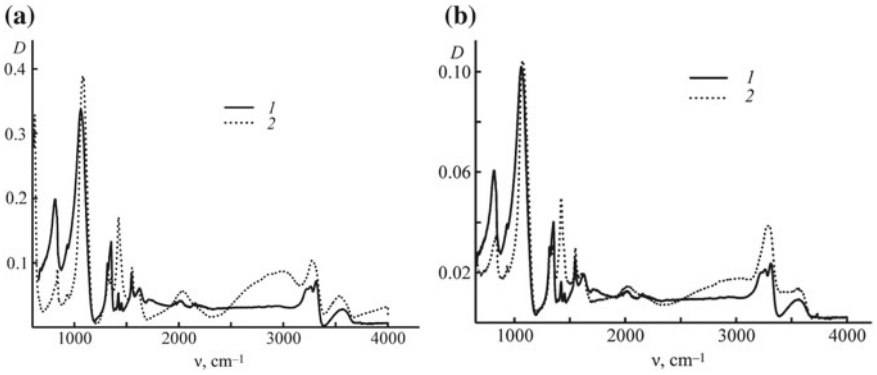

Fig. 25.9 IR spectra of NCP recorded before (1) and after (2) excitation at 470 (**a**) and 355 (**b**) nm

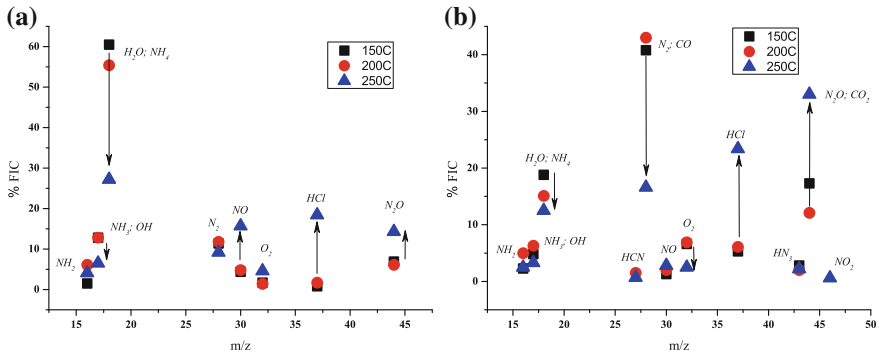

Fig. 25.10 The dependence of the proportion of ions in the whole mass spectrum on the ratio of their mass-to-charge for the products of pyrolysis of APCP (**a**) and NCP (**b**) at three temperatures. The arrows indicate the marked changes induced by the increase of the temperature of pyrolysis. The signals of HCl ions with different isotopes of chlorine are combined in one

increase of the amount of HCl (Fig. 25.10). The latter is the result of the decomposition of the perchlorate ion indicating a change in the mechanism of oxidation. Thus, the main oxidizing agents during the pyrolysis of the studied complexes at temperatures up to 200 °C are the central cobalt ion and the nitro group of 5-nitrothiazole (in the case of NCP). On the other hand, the outersphere perchlorate ion becomes the main oxidizing agent at 250 °C.

Golubev et al. performed the density functional theory (DFT) quantum-chemical calculations of the primary decomposition (with minimal energy of excitation) of NCP and BNCP using Gaussian 09 [53, 54]. The following possible primary decomposition products were calculated: ammonia, (NH_3), perchloric acid ($HClO_4$), 5-nitrotetrazolato (N_4HCNO_2), and the nitro group (NO_2). It was observed that the main primary mechanism of decomposition of both complexes is the elimination of the ammonia molecule with concurrent rearrangement of the remaining molecular fragment. At the same time, the temperature effect of this decomposition mechanism is minimal. The authors claim that the calculations are consistent with the results of mass spectrometry [55].

According to the discussion above, it can be concluded that the mechanism of low-temperature decomposition (not higher than 200 °C) corresponds to the decomposition of the complex via breaking of the weakest bonds and is similar to the photolytic decomposition of cobalt (III) amminates upon the 350 nm excitation of the d–d absorption bands, and, in opposite to high-temperature decomposition regime, is not accompanied by a significant thermal effect.

Thus, the resonance photolysis of the studied complexes conserves the perchlorate ions in the decomposition products, which can be easily detected by Raman spectroscopy. The photolysis itself is a low-temperature process that does not lead to detonation, and its solid products (cobalt oxides and hydroxides) passivate the surface of explosives [56].

25.3.1.1 Absorbing Additives

The development of nanotechnology provides new opportunities for modification of explosives. For example, the light-absorbing nanoparticles (soot, metal nanoparticles, graphene, nanotubes) are added to the explosives in order to concentrate absorbed light energy in a smaller volume [57]. Another direction is the introduction of the light-scattering nanoparticles, which extend the optical path of light in the surface layer of an explosive leading to a similar result.

It was demonstrated [58] that the addition of carbon to RDX reduces the energy of initiation compared to a pure RDX. The initiation was carried out by Nd:YAG diode pumped laser (laser power of 2.6 W and pulse duration of 200 ms) operated at 808 nm. This laser was used to study the interaction of laser radiation with HMX, RDX, PENT, and TNT, as well as their modifications with carbon (graphite, soot). Adding 1–3% carbon reduces the energy of initiation of RDX by 10–15%, probably, as noted by the authors, due to reducing the losses caused the reflection of the laser beam, which are typically about 20%.

Kalenskii et al. studied the dependence of the absorption coefficient of laser radiation (Nd:YAG, 1064 nm) of lead azide on the size of embedded lead nanoparticles [59]. It was observed that the maximum absorption coefficient (1.18) corresponds to the diameter of lead nanoparticles equals to 74 nm. The authors used the "hot spot" model in order to explain the obtained results.

The effect of the modification of the explosive compositions under the resonant laser radiation have not been previously studied. A study of the modification effect on the threshold of initiation was conducted on pressed polycrystalline samples of NCP with additions of different amounts of graphene, fullerenes (light-absorbing nanoparticles), and detonation nanodiamonds (nanoparticles with high refractive index).

At 350 nm irradiation, corresponding to d–d transitions of cobalt ion, upon reaching the threshold power the darkening of the sample surface was observed (photolytic decomposition of NCP and the formation of cobalt oxides), whereas, no explosive initiation was noticed. It was also noted that the increase in the concentration of graphene and fullerenes nanoparticles increased the threshold radiation power. This can be explained by the fact that these nanoparticles take up some part of energy and convert it into the thermal energy (Fig. 25.11b). Thus, the resulting laser power was not enough on the one hand for the photolytic initiation on the other hand, for thermal initiation, since even the radiation power (70–160 mW/mm^2) was an order of magnitude less than the required value (Fig. 25.11a).

IR spectroscopy revealed a sufficiently intense absorption band centered at 1554 nm corresponding to the first harmonic of the valence vibrations of N–H bonds. Thus, in order to observe the thermal initiation of NCP, the tunable femtosecond laser operated at 1554 nm (pulse duration of 100 fs and pulse frequency of 76 MHz) was used for the resonant excitation of this absorption band. An increase in the concentration of graphene up to 3% (in the weight percent) led to a decrease in the initiation threshold by an order of magnitude (Fig. 25.11a). This can be explained by the increase in the absorption coefficient o NCP. The further increase in the concen-

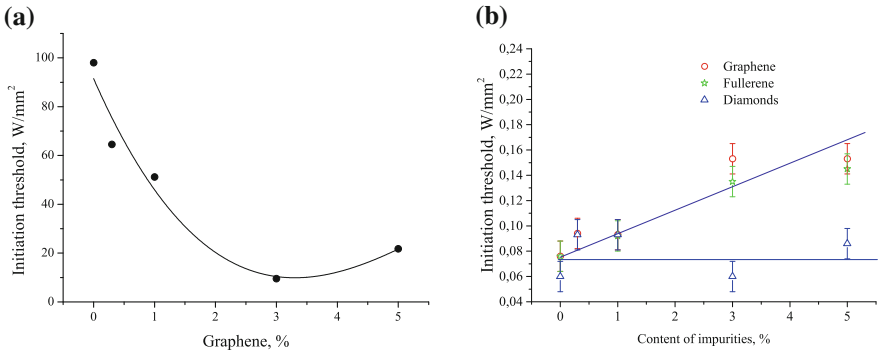

Fig. 25.11 The influence of the additives of nano-disperse materials (in wt%) on the threshold of initiation of NCP by, **a** femtosecond 1554 nm laser and, **b** Nd:YAG laser operated at 355 nm

tration of graphene led to the opposite effect, apparently, due to an increase in the outflow of a heat from the NCP layer that absorbs the bulk of the incident radiation.

25.3.1.2 Scattering Additives

The effect of additives of diffusers of light (e.g. nanodiamonds) on the explosives are poorly understood in comparison with additives based on highly absorbing nanoparticles. The use of nanodiamonds as an additive for the laser initiation of the composites based on the complex perchlorates was studied by Ilyushin et al. [57]. In this work, the composites with additives of concentrations varied between 0.5 and 5 mass% were investigated. Introduction of nanodiamonds provides sensitization of the composites with respect to laser radiation (Nd:YAG laser). The energy dependence of the initiation threshold on the additive concentration represents a curve with a minimum of about 3 mass%. The authors explain this observation by the increase of the internal optical path length of the pump radiation in the sample due to the scattering of laser radiation by ultrafine diamonds. We have studied the influence of concentration of nanodiamonds as lenses of radiation on the change in the initiation threshold at resonant excitation corresponding to the d–d of transition of cobalt ion. The obtained results showed that the modification of NCP perchlorate by detonation nanodiamonds did not affect the magnitude of the threshold power (Fig. 25.11b). Apparently, this is due to the fact that the increase in the length of the optical path as a result of the scattering effect of such additives is critical only for materials with a low optical absorption coefficient.

25.4 Conclusions

Modern directions in the field of the explosive treatment by laser light lie in an investigation of the interactions between the resonant laser radiation and the absorbing and scattering light nanoparticles used as additives to explosives, and affecting the initiation threshold. The implementation of this approach to cobalt (III) nitrotetrazolato amminates allowed us to obtain the following results. For these compounds, three groups of resonance absorption bands have been established: the first group—the overtones of valence vibrations at wavelengths of 1.5 and more than 2 μm; the second group—two absorption bands corresponding to d–d transitions of cobalt ion located in the region of 300–500 nm, and the third group—the charge transfer of ligand-to-metal absorption band located in the short-wavelength region. Photolytic decomposition of the aforementioned complexes was carried out using laser radiation. It was found that irradiation of cobalt (III) amminates at 355 and 470 nm, corresponding to d–d transitions of cobalt ion, leads to "soft" photolytic decomposition providing the conditions for passivation of the surface of the explosives. In this scenario, perchlorate anion as one of the decomposition products is produced, which can be easily detected and identified. Addition to NCP of the highly absorbing carbon nanoparticles allows to significantly reduce the initiation threshold at the wavelengths corresponding to the valence vibrations.

Acknowledgements This work was supported by the Russian Foundation for Basic Research, project no. 16-29-01056-ofi_m. Measurements were partly made at the resource center of St. Petersburg State University "Optical and Laser Methods for Analysis of Substances".

References

1. M.J. Gifford, W.G. Proud, J.E. Field, Development of a method for qualification of hot-spots. Thermochim. Acta **384**, 285–290 (2002)
2. Y.-C. Liau et al., Laser-induced ignition of RDX monopropellant. Combust. Flame **126**, 1680–1698 (2001)
3. J.M. McAfee, The deflagration to detonation transition, in *Shock Wave Science and Technology Reference Library. 5: Non-Shock Initiation of Explosives*, ed. by B.W. Asay (Springer, Berlin, 2010), pp. 483–535
4. M.D. Furnish, N.N. Thadhani, Y. Horie, Am. Inst. Phys. (Melville, NY) 878–881 (2002)
5. M.S. Abdulazeem et al., Int. J. Therm. Sci. **50**, 2117–2121 (2011)
6. S. Ruiqi, W. Lizhi, Z. Wei, Z. Haonan, Laser ablation of energetic materials, in *Laser Ablation—From Fundamentals to Applications*. http://dx.doi.org/10.5772/intechopen.71892
7. L.A. Skvortsov, Laser methods for detection of the explosives traces on the surfaces of distant objects. Quantum Electron. **42**(1) (2012)
8. L.A. Skvortsov, E.M. Maksimov, Quantum Electron. **40**(7), 565 (2010)
9. D. Kremers, L. Radziemsky, *Laser-Indused Breakdown Spectroscopy* (Technosphere, Moscow, 2009)
10. A. Popov, T. Labutin, N. Zorov, Mosc. Univ. Chem. Bull. **50**(6), 453 (2009)
11. F. De Lucia, A. Samuels, R. Harmon, R. Walters, K. McNesby, A. LaPointe, R. Winkel, A. Miziolek, IEEE Sens. J. **5**, 681 (2005)

12. J. Gottfried, F.D. Lucia, C.J. Munson, A. Miziolek, Anal. Bioanal. Chem. **395**, 283 (2009)
13. V. Demtreder, *Laser Spectroscopy. Basic Principles and Experimental Technique* (Science, Moscow, 1985)
14. S. Sharma, P. Lucey, M. Ghosh, H. Hubble, K. Horton, Spectrochim. Acta A **59**, 2391 (2003)
15. J. Carter, J. Scaffidi, S. Burnett, B. Vasser, S. Sharma, S. Angel, Spectrochim. Acta A **61**, 2288 (2005)
16. D. Tuschel, A. Mikholin, B. Lemoff, S. Asher, Appl. Spectrosc. **64**(4), 425 (2010)
17. K.L. Gares et al., Review of explosive detection methods and the emergence of standoff deep UV resonance Raman. J. Raman Spectrosc. **47**, 124–141 (2016)
18. B.H. Hokra et al., Single-shot stand-off chemical identification of powers using random Raman lasing. PNAS **111**(34), 12320–12324 (2014)
19. S.A. Ahmanov, N.I. Koroteev, UFN **123**, 405 (1977)
20. T. Arusi-Parpar, D. Heflinger, R. Lavi, Appl. Opt. **40**, 6677 (2001)
21. T. Arusi-Parpar, R. Lavi, Remote detection of explosives by enhanced pulsed laser photodissotiation/laser-induced fluorescence method, in *Paper Presented at the NA TO Advanced Research Workshop on Stand-off Detection of Suicide Bombers and Mobile Subjects Pfinztal* (2006), pp. 13–14
22. C. Wynn, S. Palmacci, R. Kunz, M. Rothshild, Lincoln Lab. J. **17**(2), 27 (2008)
23. C. Wynn, R. Palmacci, K. Kunz, K. Clow, M. Rothshild, Proc. SPIE Int. Soc Opt. Eng. **6954**, 695407 (2008)
24. C. Wynn, R. Palmacci, K. Kunz, K. Clow, M. Rothshild, Appl. Opt. **37**(31), 5767 (2008)
25. J. White, F. Akin, H. Oser, R. Crosley, Appl. Opt. **50**(1), 74 (2011)
26. C. Bauer, P. Geiser, J. Burgmeier, J. Holl, W. Schade, Appl. Phys. B Lasers Opt. **85**, 251 (2006)
27. C. Bauer, J. Burgmeier, C. Bohling, W. Schade, J.C. Holl, in *Proceedings of the NATO Advanced Research Workshop on Stand-off Detection of Suicide-Bombers and Mobile Subjects* (Springer, The Netherlands, 2006), p. 27
28. U. Willer, M. Saraji, A. Khorsandi, P. Geisher, W. Schade, Opt. Lasers Eng. **44**, 699 (2006)
29. C. Bauer, A. Sharma, U. Willer, J. Burgmeier, B. Braunschweig, W. Schade, S. Blaser, L. Hvozdara, A. Mfffler, G. Holl, Appl. Phys. B **92**(3), 327 (2008)
30. C. Bauer, U. Willer, W. Schade, Opt. Eng. **49**, 111126 (2010)
31. D. Edward, A. Krechetov, A. Mitrofanov, D. Nurmukhametov, M. Kuklja, J. Phys. Chem. C **115**, 6893–6901 (2011)
32. Y. Sun, X. Tao, Y. Shu, F. Zhong, UV-induced photodecomposition of 2,2′, 4,4′, 6,6′-hexanitrostillbene (HNS), Mater. Sci.-Pol. **31**(3), 306–311 (2013), http://www.materialsscience.pwr.wroc.pl/. https://doi.org/10.2478/s13536-013-0105-9
33. S. Kakar et al., Phys. Rev. B. **62**, 15666 (2000)
34. J.W. McDonald et al., J. Energ. Mater. **19**, 101 (2001)
35. A.S. Tverjanovich, A.O. Averyanov, M.A. Ilyushin, YuS Tverjanovich, A.V. Smirnov, Effect of laser radiation on tetrazolate ammine cobalt III complexes. Bull. SpbSIT (TU) **26**(52), 3–7 (2014)
36. A.S. Tverjanovich, A.O. Averyanov, M.A. Ilyushin, YuS Tverjanovich, A.V. Smirnov, The Raman spectra of nitrotetrazolo(lato) ammine cobalt III perchlorates. Bull. SpbSIT (TU) **27**(53), 8–10 (2014)
37. A.S. Tverjanovich et al., Universum. **12**(19) (2015)
38. Int. J. Energ. Mater. Chem. Propuls. **15**(2), 113–122 (2016)
39. G.O. Abdrashitov, A.O. Aver'yanov, M.D. Bal'makov, M.A. Ilyushin, A.S. Tverjanovich, Yu.S. Tver'yanovich, Decomposition of Pentaammineaquacobalt (III) Perchlorate under laser radiation action. Russ. J. Gen. Chem. **87**(7), 1451–1455 (2017)
40. M.A. Ilyushina, Yu.S. Tverjanovich, A.S. Tverjanovich, A.O. Aver'yanov, A.V. Smirnov, I.V. Shugalei, On the mechanism of Cobalt(III) aminates pyrolysis. Russ. J. Gen. Chem. **87**(11), 2600–2604 (2017)
41. A.S. Tverjanovicha, A.O. Aver'yanov, M.A. Ilyshin, Yu.S. Tverjanovich, A.V. Smirnov, Decomposition of Cobalt(III) Nitrotetrazolato Amminates under the action of laser light. Russ. J. Gen. Chem. **88**(2), 226–231 (2017)

42. M.A. Ilyushin, A.V. Smirnov, V.N. Andreev, I.V. Tselinskii, I.V. Shugalei, O.M Nesterova. Russ. J. Gen. Chem. **85**(13), 1620 (2015)
43. A.V. Smirnov, M.A. Ilyushin, I.V. Tselinskii, Synthesis of Cobalt(III) Ammine complexes as explosives for safe taking charges. Russ. J. Appl. Chem. **77**(5), 794–796 (2004)
44. M.A. Ilyushin, A.M. Sudarikov, I.V. Tselinskii, *Metallic Complexes in High-Energy Materials* (LGU im A. S. Pushkina Publ., St. Petersburg, 2010), p. 188
45. M.A. Ilyushin, I.V. Tselinskii, A.A. Kotomin, *High Power Substances for Arsenal of Initiation* (SPbGTI (TU) Publ., St. Petersburg, 2013), p. 176
46. Int. J. Energ. Mater. Chem. Propuls. **15**(2), 113–122 (2016)
47. Eng. J. Gun. Than. **88**(2) (2017)
48. JTh Kloprogge, D. Wharton, L. Hickey et al., Infrared and Raman study of interlayer anions CO_3^{2-}, NO_3^{-}, SO_4^{2-} and ClO_4^{-} in Mg/Al-hydrotalcite. Am. Miner. **87**(5–6), 623–629 (2002)
49. E. Ingier-Stocka, M. Maciejewski, Thermal decomposition of $[Co(NH_3)_6]_2(C_2O_4)_3{\cdot}4H_2O$: I. Identification of the solid products. Thermochim. Acta. **354**, 45–57 (2000)
50. E. Mikulia, A. Migdal-Mikulia, N.S. Gorskaa Wrobelb, J. Sciesinskic, E. Sciesinskac, Phase transition and molecular motions in $[Co(MH_3)_6](ClO_4)_3$ studied by differential scanning calorimetry and infrared spectroscopy. J. Mol. Struct. 651–653 (2003)
51. Sigma-Aldrich, Catalog of Raman spectra, Hexamminecobalt (III) chloride (2012)
52. H.A. Block, Vibrational study of the hexamminecobalt (III) ion. Trans. Faraday Soc. **55**, 867–875 (1959)
53. V.K. Golubev, M.A. Ilyushin, The primary mechanism of decomposition of nitrotetrazolium of cobalt(III)//Doha. **87**(2), 312 (2017)
54. V.K. Golubev, M.A. Ilyushin, Primary decomposition mechanism of Cobalt (III) Nitrotetrazolatoammine complexes. Russ. J. Gen. Chem. **87**, 286 (2017)
55. A.S. Tverjanovich, A.O. Aver'yanov, M.A. Ilyushin, YuS Tverjanovich, A.V. Smirnov, Russ. J. Appl. Chem. **88**(2), 226 (2015)
56. A.S. Tverjanovich, e.a. Patent RF 2636525 (2016)
57. M.A. Ilyushin et al., Effect of additives of ultra fine carbon particles on the laser initiation threshold of a polymer is a photosensitive explosive composition. Chem. Fiz **24**(10), 49–56 (2005)
58. M. Harkoma, Confinement in the diode laser ignition of energetic materials, Thesis for the degree of Doctor of Technology to be presented with due permission for public examination and criticism in Sahkotalo Building, Auditorium S1, at Tampere University of Technology, 2010
59. A.V. Kalenskii et al., Paradox of small particles in the pulsed laser initiation of explosive decomposition. Combust. Explos. Shock. Waves **52**(2), 234–240 (2016)